Supporting Information

Synthesis, Crystal Structure, and Physical Properties of the Eu(II)-Based Selenide Semiconductor: $EuHfSe_3$

Subhendu Jana,[1] Shaun O'Donnell,[2] Ian A. Leahy,[2] Aylin Koldemir,[3] Rainer Pöttgen,[3] Rebecca W. Smaha,[2] and Paul A. Maggard[1,*]

[1] *Department of Chemistry, North Carolina State University, Raleigh, North Carolina, USA, 27695.*

[2] *Materials Science Center, National Renewable Energy Laboratory, Golden, Colorado, USA, 80401.*

[3] *Institut für Anorganische und Analytische Chemie, Universität Münster, Corrensstrasse 30, 48149 Münster, Germany.*

*Corresponding author e-mail: Paul_Maggard@ncsu.edu

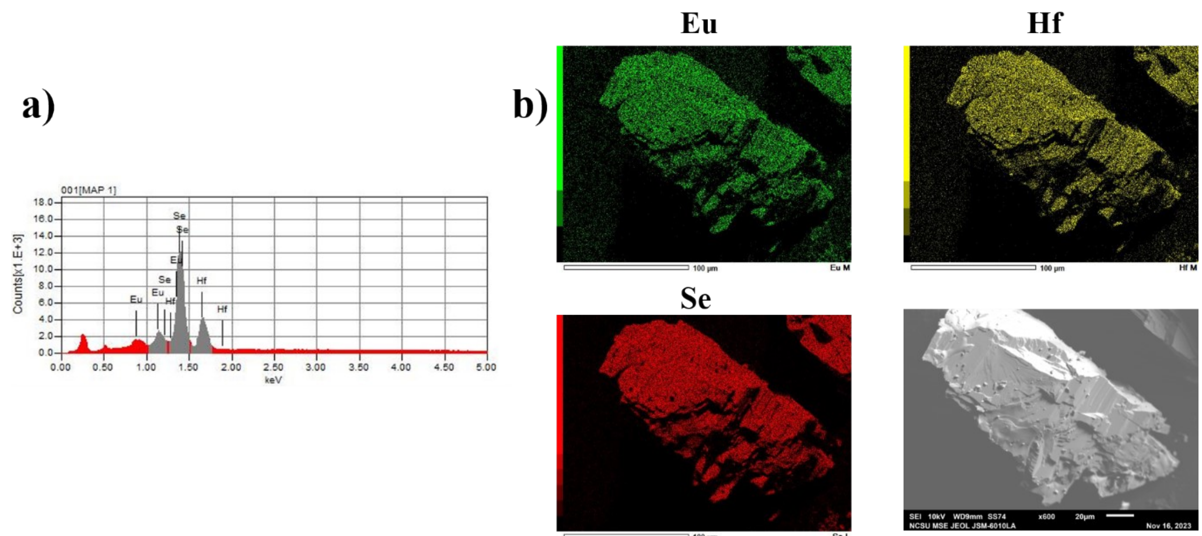

Figure S1. (a) EDX analysis and (b) elemental mapping of selected $EuHfSe_3$ crystals. The observed elemental percentages of Eu, Hf, and Se are 17.6%, 21.0%, and 61.4%, respectively.

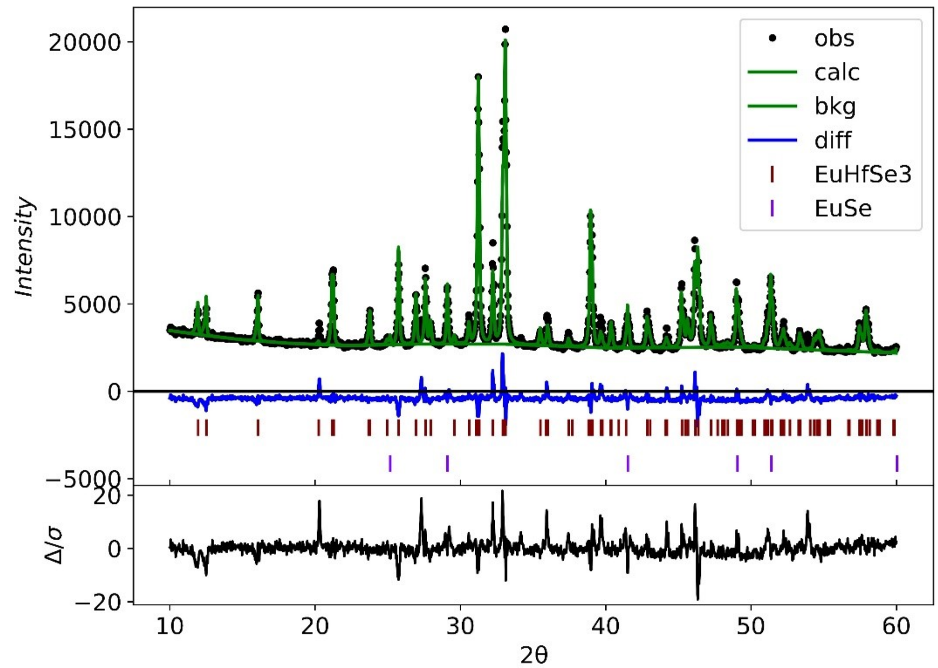

Figure S2. Rietveld refinement of powder x-ray diffraction data of $EuHfSe_3$ and a EuSe secondary phase (wR: 5.231%). The calculated phase fractions were 89.13 wt% $EuHfSe_3$ and 10.87 wt% EuSe.

Table S1. Atomic displacement parameters (Å^2) for the refined $EuHfSe_3$ structure.

Atom	U^{11}	U^{22}	U^{33}	U^{12}	U^{13}	U^{23}
Eu1	0.0228(2)	0.01082(19)	0.0157(2)	0.000	-0.00069(17)	0.000
Hf1	0.01207(18)	0.00974(17)	0.0124(2)	0.000	0.00032(12)	0.000
Se1	0.0107(4)	0.0093(3)	0.0089(4)	0.000	-0.0001(3)	0.000
Se2	0.0103(4)	0.0082(3)	0.0141(4)	0.000	0.0019(3)	0.000
Se3	0.0136(4)	0.0109(4)	0.0113(4)	0.000	0.0025(3)	0.000

Table S2. Selected metric variables (Å and º) for the refined $EuHfSe_3$ crystal structure.

Eu1—Se3^{i}	3.1568 (7)	Eu1—Eu1^{vii}	3.9300 (4)
Eu1—Se3^{ii}	3.1568 (7)	Eu1—Eu1^{viii}	3.9300 (4)
Eu1—Se1^{iii}	3.1664 (9)	Hf1—Se3	2.5572 (9)
Eu1—Se2^{iv}	3.2053 (8)	Hf1—Se2^{v}	2.6729 (6)
Eu1—Se2^{v}	3.2053 (8)	Hf1—Se2^{iv}	2.6729 (6)
Eu1—Se3^{iv}	3.2069 (8)	Hf1—Se1^{ix}	2.6963 (6)
Eu1—Se3^{v}	3.2069 (7)	Hf1—Se1^{x}	2.6963 (6)
Eu1—Se2^{vi}	3.3617 (9)	Hf1—Se1	2.7214 (9)
Se3^{i}—Eu1—Se3^{ii}	76.99 (2)	Se2^{vi}—Eu1—Eu1^{viii}	90.0
Se3^{i}—Eu1—Se1^{iii}	69.21 (2)	Eu1^{vii}—Eu1—Eu1^{viii}	180.0
Se3^{ii}—Eu1—Se1^{iii}	69.21 (2)	Se3—Hf1—Se2^{v}	95.76 (2)
Se3^{i}—Eu1—Se2^{iv}	136.69 (2)	Se3—Hf1—Se2^{iv}	95.76 (2)
Se3^{ii}—Eu1—Se2^{iv}	87.963 (18)	Se2^{v}—Hf1—Se2^{iv}	94.64 (3)
Se1^{iii}—Eu1—Se2^{iv}	141.634 (12)	Se3—Hf1—Se1^{ix}	90.91 (2)
Se3^{i}—Eu1—Se2^{v}	87.963 (18)	Se2^{v}—Hf1—Se1^{ix}	173.28 (3)
Se3^{ii}—Eu1—Se2^{v}	136.69 (2)	Se2^{iv}—Hf1—Se1^{ix}	85.504 (18)
Se1^{iii}—Eu1—Se2^{v}	141.634 (12)	Se3—Hf1—Se1^{x}	90.91 (2)
Se2^{iv}—Eu1—Se2^{v}	75.62 (2)	Se2^{v}—Hf1—Se1^{x}	85.504 (18)
Se3^{i}—Eu1—Se3^{iv}	141.159 (16)	Se2^{iv}—Hf1—Se1^{x}	173.28 (3)
Se3^{ii}—Eu1—Se3^{iv}	90.921 (11)	Se1^{ix}—Hf1—Se1^{x}	93.57 (3)
Se1^{iii}—Eu1—Se3^{iv}	71.98 (2)	Se3—Hf1—Se1	175.67 (3)
Se2^{iv}—Eu1—Se3^{iv}	78.243 (19)	Se2^{v}—Hf1—Se1	87.17 (2)
Se2^{v}—Eu1—Se3^{iv}	123.20 (2)	Se2^{iv}—Hf1—Se1	87.17 (2)
Se3^{i}—Eu1—Se3^{v}	90.921 (11)	Se1^{ix}—Hf1—Se1	86.13 (2)
Se3^{ii}—Eu1—Se3^{v}	141.159 (16)	Se1^{x}—Hf1—Se1	86.13 (2)
Se1^{iii}—Eu1—Se3^{v}	71.984 (19)	Hf1^{ix}—Se1—Hf1^{x}	93.57 (3)
Se2^{iv}—Eu1—Se3^{v}	123.20 (2)	Hf1^{ix}—Se1—Hf1	93.87 (2)
Se2^{v}—Eu1—Se3^{v}	78.243 (19)	Hf1^{x}—Se1—Hf1	93.87 (2)
Se3^{iv}—Eu1—Se3^{v}	75.58 (2)	Hf1^{ix}—Se1—Eu1^{xi}	97.03 (2)
Se3^{i}—Eu1—Se2^{vi}	72.98 (2)	Hf1^{x}—Se1—Eu1^{xi}	97.03 (2)
Se3^{ii}—Eu1—Se2^{vi}	72.98 (2)	Hf1—Se1—Eu1^{xi}	164.04 (3)

$Se1^{iii}$—Eu1—$Se2^{vi}$	131.07 (2)	$Hf1^{xii}$—Se2—$Hf1^{xiii}$	94.64 (3)
$Se2^{iv}$—Eu1—$Se2^{vi}$	63.78 (2)	$Hf1^{xii}$—Se2—$Eu1^{xii}$	88.897 (12)
$Se2^{v}$—Eu1—$Se2^{vi}$	63.78 (2)	$Hf1^{xiii}$—Se2—$Eu1^{xii}$	151.90 (3)
$Se3^{iv}$—Eu1—$Se2^{vi}$	138.718 (13)	$Hf1^{xii}$—Se2—$Eu1^{xiii}$	151.90 (3)
$Se3^{v}$—Eu1—$Se2^{vi}$	138.718 (13)	$Hf1^{xiii}$—Se2—$Eu1^{xiii}$	88.897 (12)
$Se3^{i}$—Eu1—$Eu1^{vii}$	51.504 (11)	$Eu1^{xii}$—Se2—$Eu1^{xiii}$	75.62 (2)
$Se3^{ii}$—Eu1—$Eu1^{vii}$	128.497 (11)	$Hf1^{xii}$—Se2—$Eu1^{xiv}$	91.58 (2)
$Se1^{iii}$—Eu1—$Eu1^{vii}$	90.0	$Hf1^{xiii}$—Se2—$Eu1^{xiv}$	91.58 (2)
$Se2^{iv}$—Eu1—$Eu1^{vii}$	127.809 (11)	$Eu1^{xii}$—Se2—$Eu1^{xiv}$	116.22 (2)
$Se2^{v}$—Eu1—$Eu1^{vii}$	52.190 (11)	$Eu1^{xiii}$—Se2—$Eu1^{xiv}$	116.22 (2)
$Se3^{iv}$—Eu1—$Eu1^{vii}$	127.788 (11)	Hf1—Se3—$Eu1^{i}$	98.68 (2)
$Se3^{v}$—Eu1—$Eu1^{vii}$	52.212 (11)	Hf1—Se3—$Eu1^{ii}$	98.68 (2)
$Se2^{vi}$—Eu1—$Eu1^{vii}$	90.0	$Eu1^{i}$—Se3—$Eu1^{ii}$	76.99 (2)
$Se3^{i}$—Eu1—$Eu1^{viii}$	128.497 (11)	Hf1—Se3—$Eu1^{xiii}$	98.99 (2)
$Se3^{ii}$—Eu1—$Eu1^{viii}$	51.504 (11)	$Eu1^{i}$—Se3—$Eu1^{xiii}$	162.31 (3)
$Se1^{iii}$—Eu1—$Eu1^{viii}$	90.0	$Eu1^{ii}$—Se3—$Eu1^{xiii}$	100.948 (10)
$Se2^{iv}$—Eu1—$Eu1^{viii}$	52.190 (11)	Hf1—Se3—$Eu1^{xii}$	98.99 (2)
$Se2^{v}$—Eu1—$Eu1^{viii}$	127.809 (11)	$Eu1^{i}$—Se3—$Eu1^{xii}$	100.948 (10)
$Se3^{iv}$—Eu1—$Eu1^{viii}$	52.212 (11)	$Eu1^{ii}$—Se3—$Eu1^{xii}$	162.31 (3)
$Se3^{v}$—Eu1—$Eu1^{viii}$	127.788 (11)	$Eu1^{xiii}$—Se3—$Eu1^{xii}$	75.58 (2)

Symmetry codes: (i) -*x*+1, -*y*+1, -*z*+1; (ii) -*x*+1, -*y*, -*z*+1; (iii) *x*+1/2, -*y*+1/2, -*z*+3/2; (iv) -*x*+1/2, *y*-1/2, *z*+1/2; (v) -*x*+1/2, *y*+1/2, *z*+1/2; (vi) *x*+1/2, -*y*+1/2, -*z*+1/2; (vii) *x*, *y*+1, *z*; (viii) *x*, *y*-1, *z*; (ix) -*x*, -*y*, -*z*+1; (x) -*x*, -*y*+1, -*z*+1; (xi) *x*-1/2, -*y*+1/2, -*z*+3/2; (xii) -*x*+1/2, *y*+1/2, *z*-1/2; (xiii) -*x*+1/2, *y*-1/2, *z*-1/2; (xiv) *x*-1/2, -*y*+1/2, -*z*+1/2.

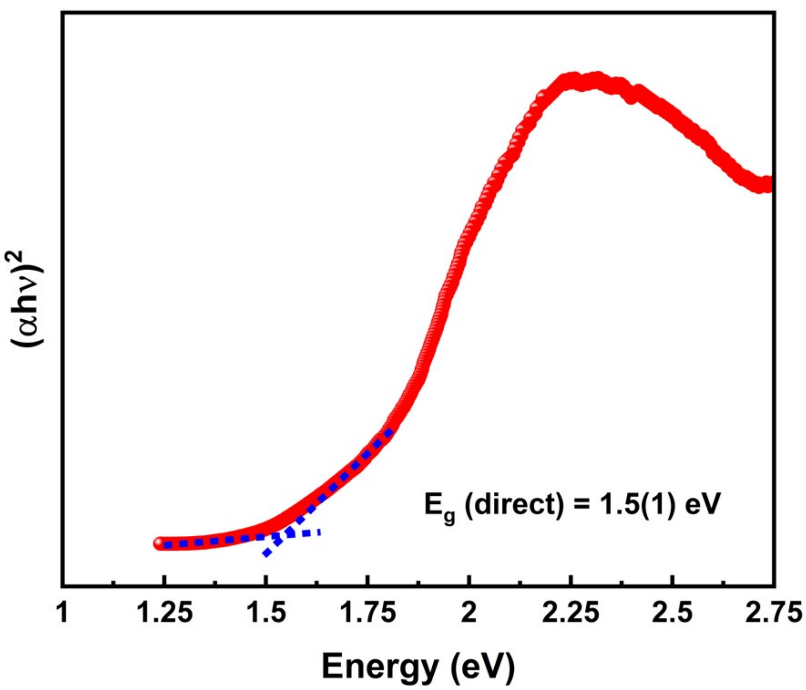

Figure S3. Plot of the UV-Vis diffuse reflectance spectrum of the polycrystalline $EuHfSe_3$ powder.

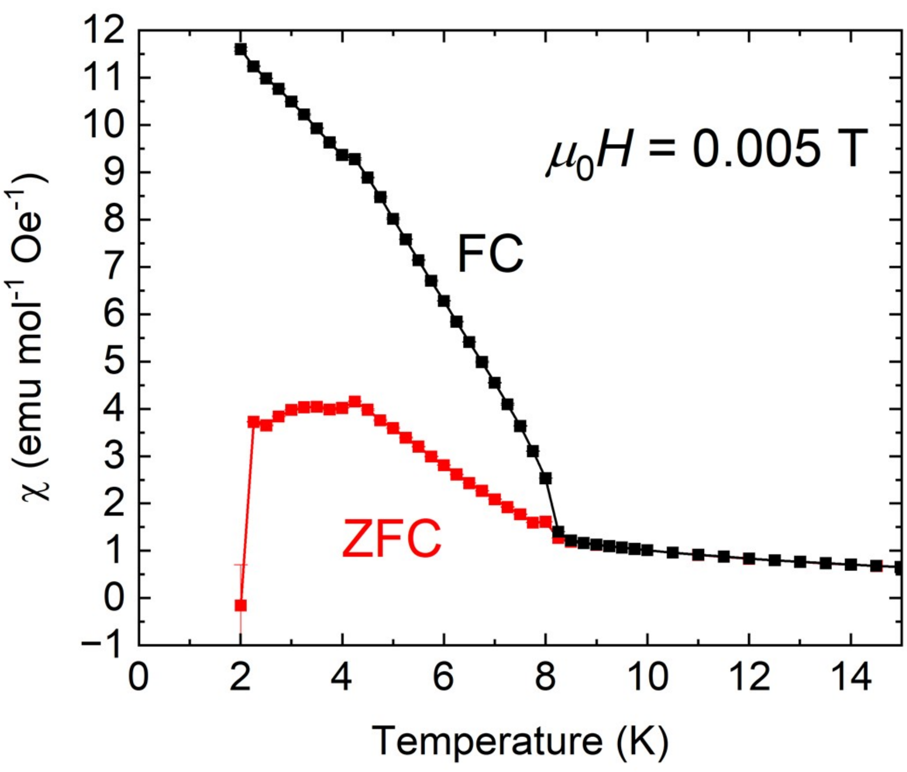

Figure S4. Zero-field-cooled (ZFC) and field-cooled (FC) magnetic susceptibility (χ) as a function of temperature collected at an applied field of $\mu_0 H = 0.005$ T.

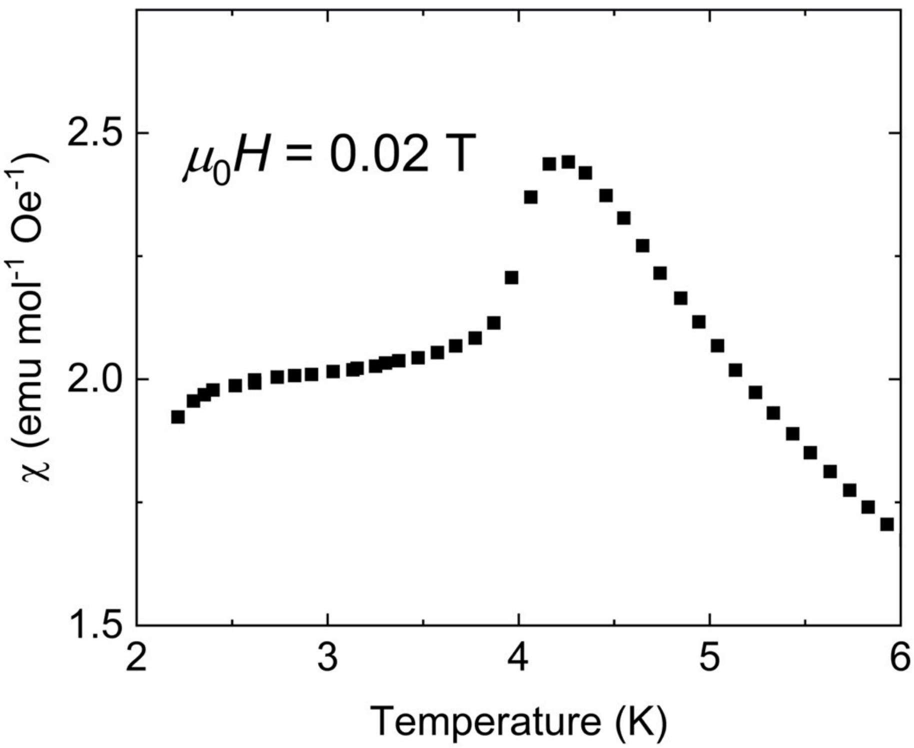

Figure S5. ZFC magnetic susceptibility (χ) as a function of temperature collected at an applied field of $\mu_0H = 0.02$ T.

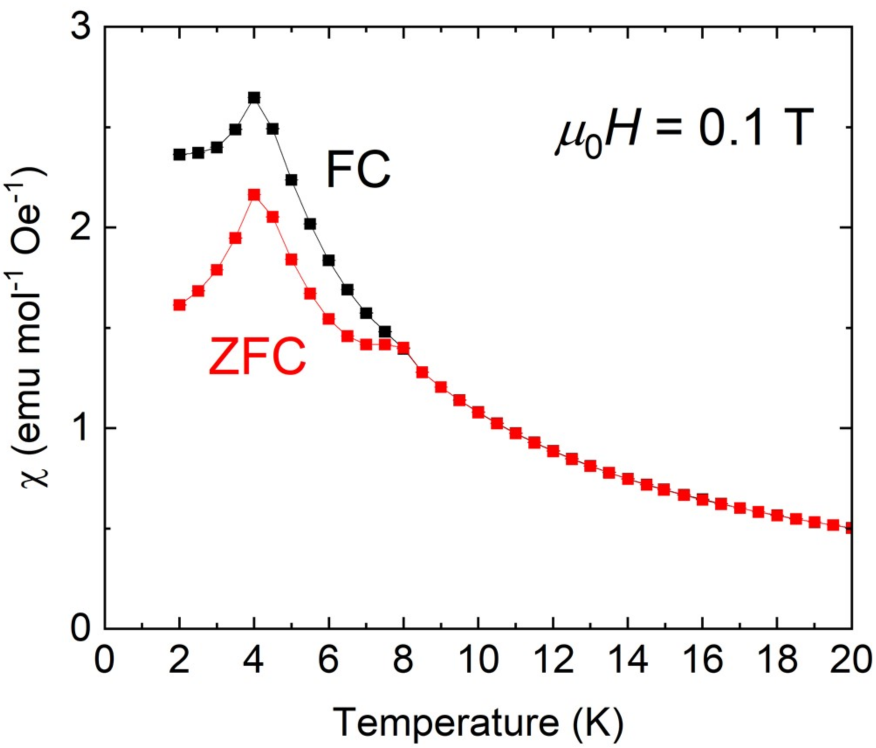

Figure S6. ZFC and FC magnetic susceptibility (χ) as a function of temperature collected at an applied field of $\mu_0H = 0.1$ T.

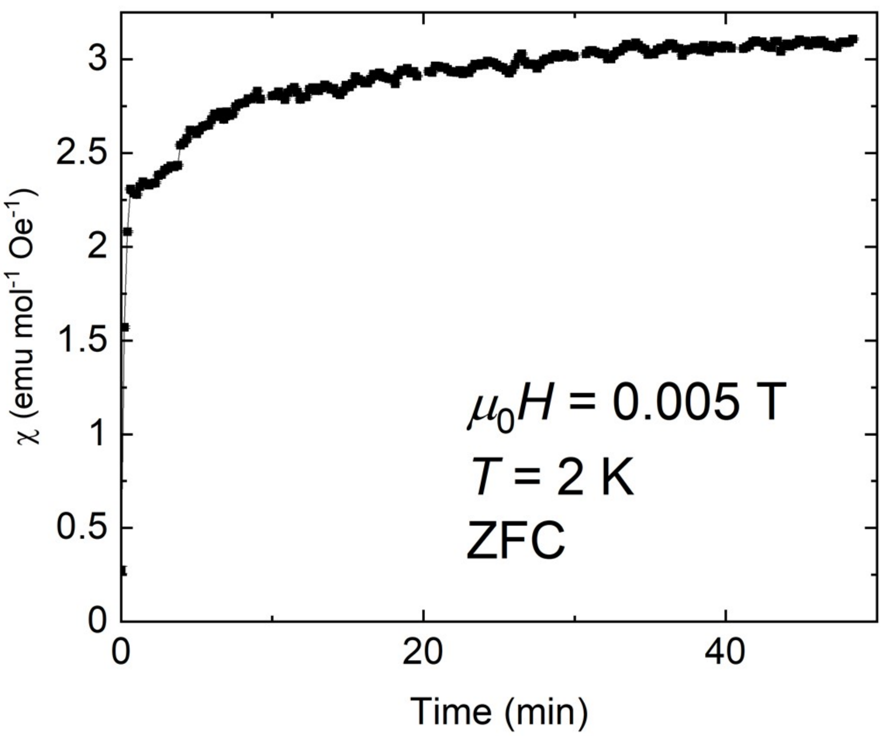

Figure S7. Magnetic susceptibility as a function of measurement time collected in an applied field of μ_0H = 0.005 T.

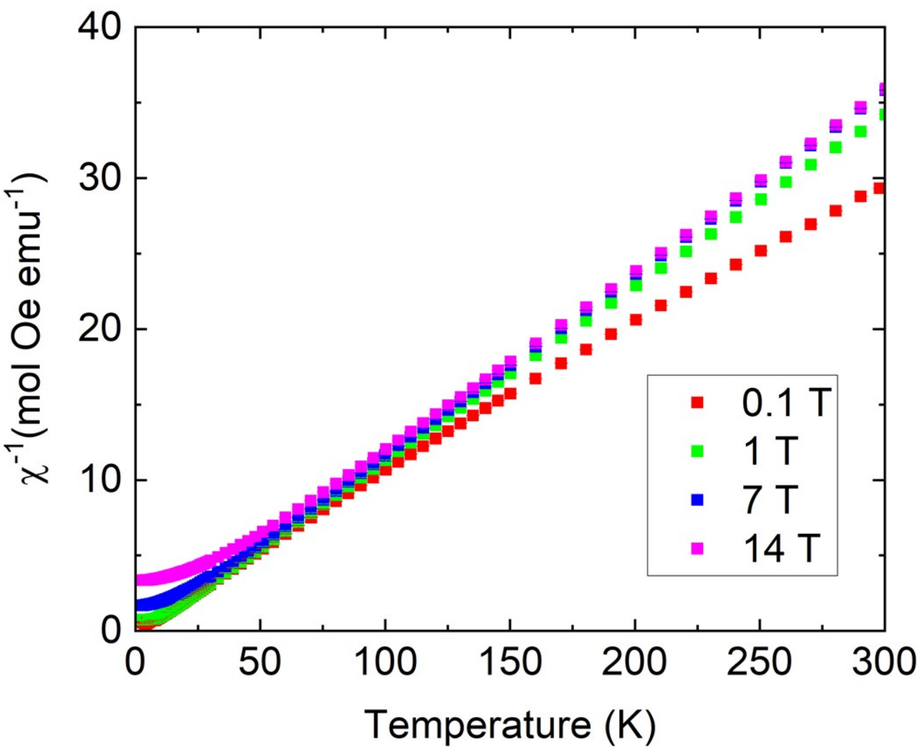

Figure S8. Inverse magnetic susceptibility (χ^{-1}) as a function of temperature at several applied fields.

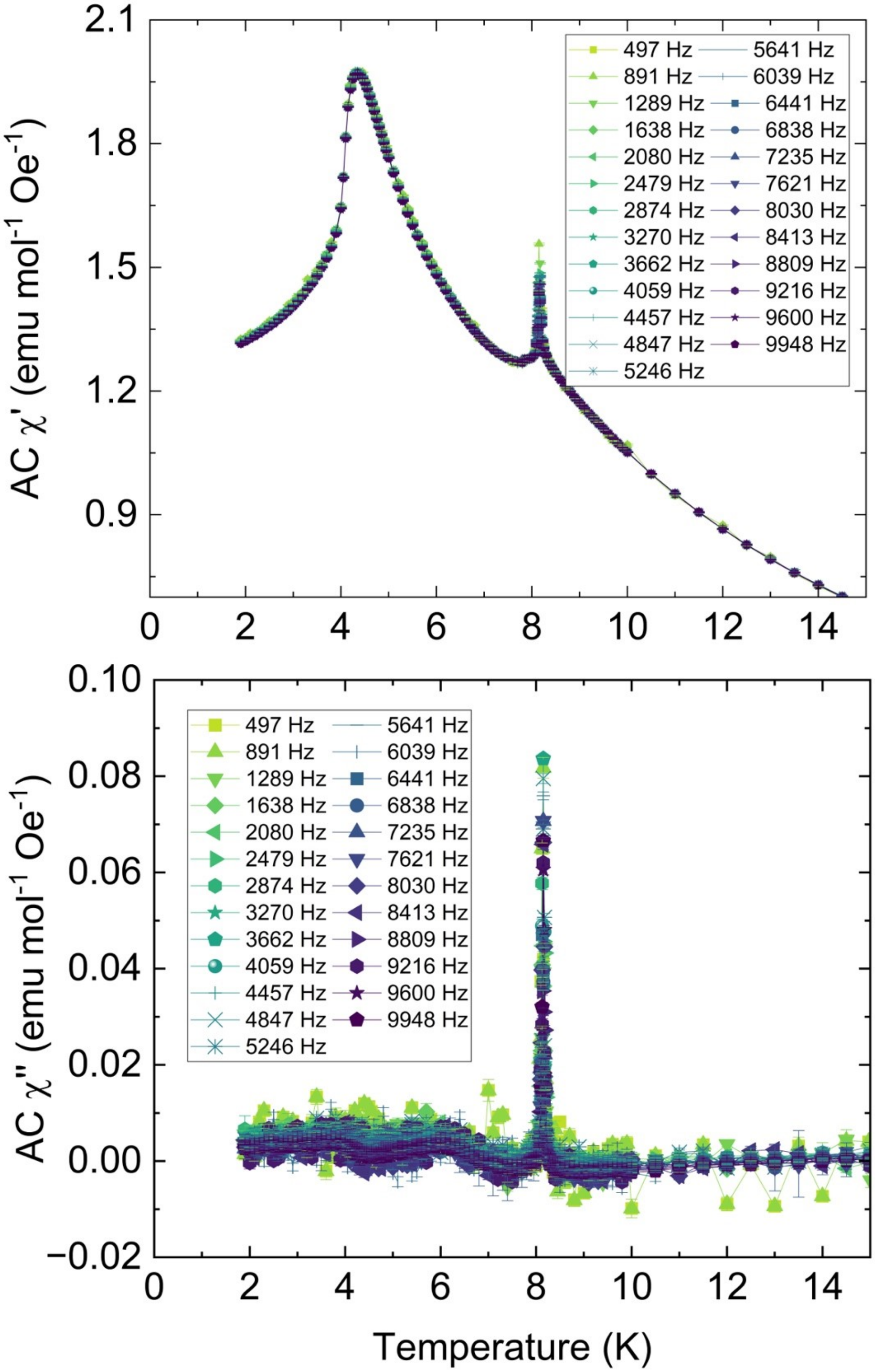

Figure S9. Frequency dependence of the real (χ') and imaginary (χ'') parts of the AC susceptibility measured in zero applied field.

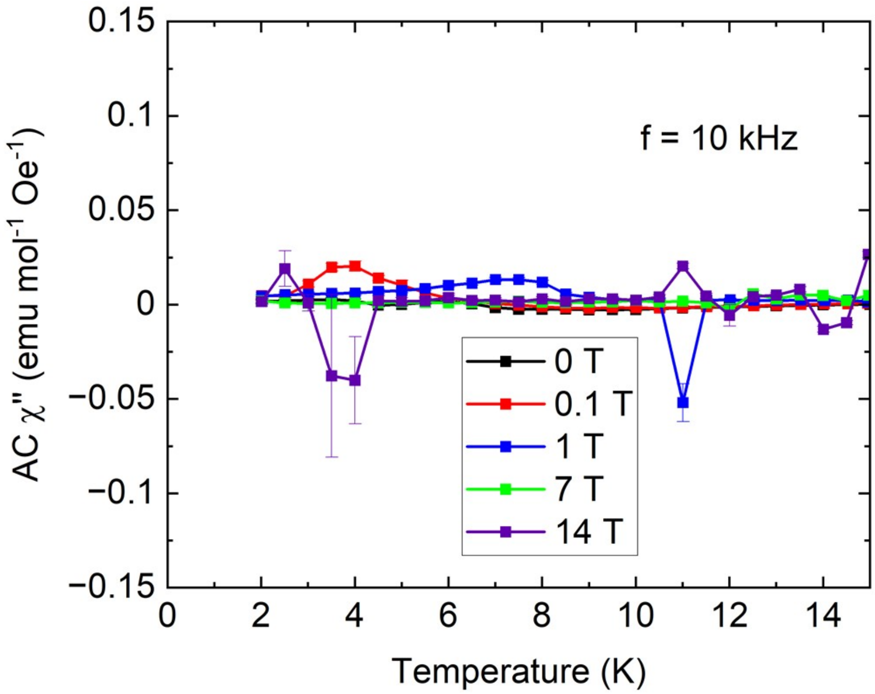

Figure S10. Temperature dependence of the imaginary part of the AC susceptibility (χ'') measured at several applied fields.

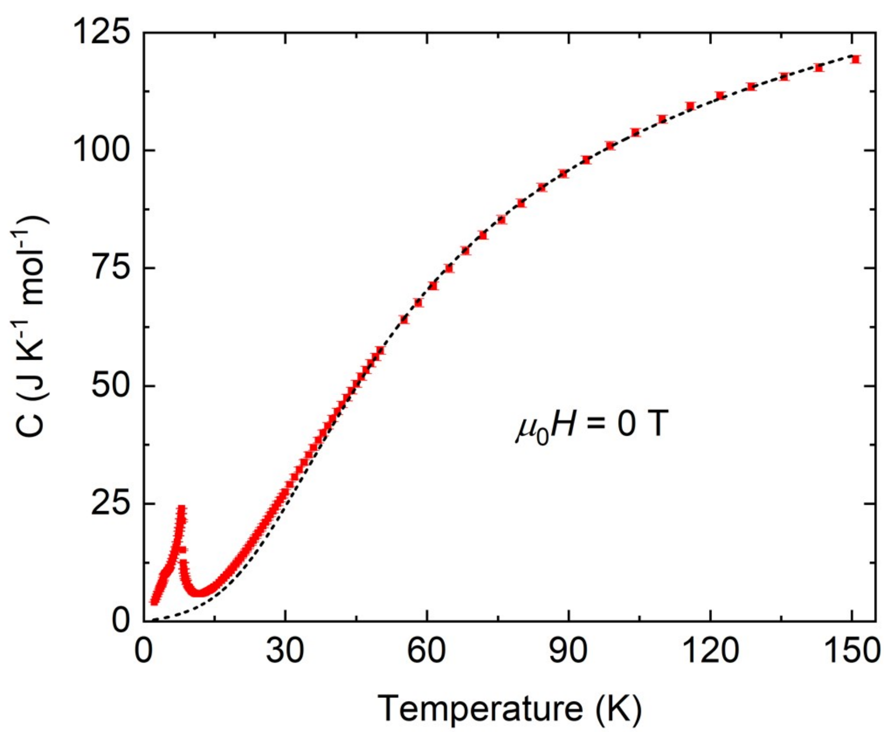

Figure S11. Molar heat capacity (C_p) measured at μ_0H = 0 T. The dashed line indicates the background (C_{bg}) extrapolated to T = 0 K; see the main text for details.

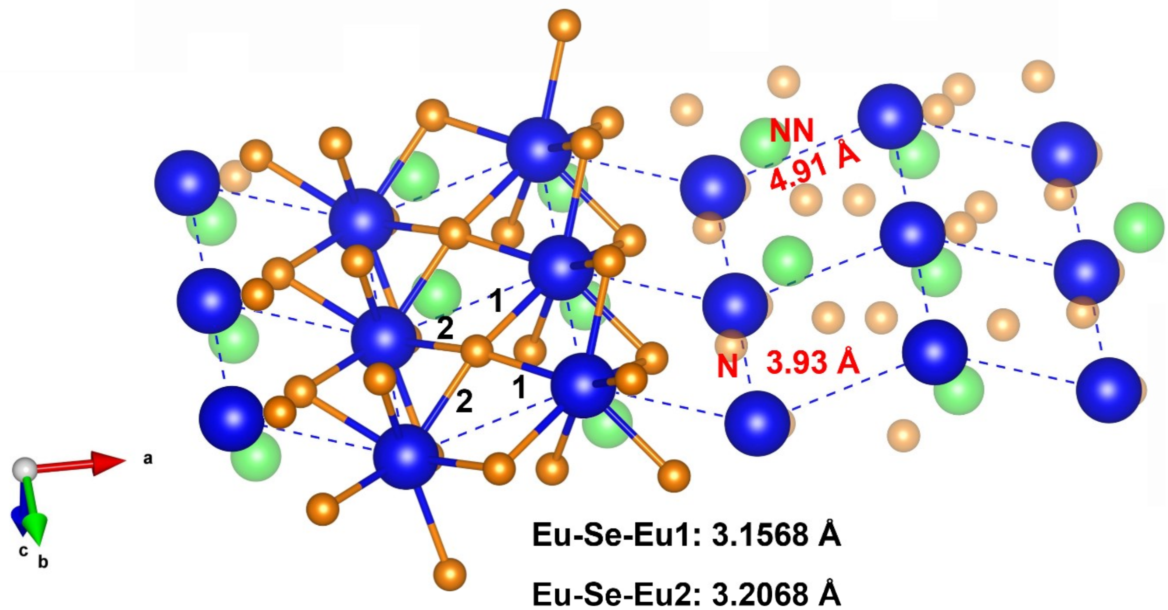

Figure S12. Structural view of the corrugated [$EuSe_2Se_{2/2}Se_{4/4}$] layer with Eu-Eu nearest-neighbor distances shown in each direction as dashed lines.